The Effect of Stimulation Intensity, Sampling Frequency, and Sample Synchronization in TMS-EEG on the TMS Pulse Artifact Amplitude and Duration

Zunaira Jamil, Laura Säisänen, Michal Demjan, Jusa Reijonen, and Petro Julkunen

***Abstract*— Transcranial magnetic stimulation (TMS) coupled with electroencephalography (EEG) possesses diagnostic and therapeutic benefits. However, TMS provokes a large pulse artifact that momentarily obscures the cortical response, presenting a significant challenge for EEG data interpretation. We examined how stimulation intensity (SI), EEG sampling frequency (Fs) and synchronization of stimulation with EEG sampling influence the amplitude and duration of the pulse artifact. In eight healthy subjects, single-pulse TMS was administered to the primary motor cortex, due to its well-documented responsiveness to TMS. We applied two different SIs (90% and 120% of resting motor threshold, representing the commonly used subthreshold and suprathreshold levels) and Fs (conventional 5 kHz and high frequency 20 kHz) both with TMS synchronized with the EEG sampling and the conventional non-synchronized setting. Aside from removal of the DC-offset and epoching, no preprocessing was performed to the data. Using a random forest regression model, we identified that Fs had the largest impact on both the amplitude and duration of the pulse artifact, with median variable importance values of 1.444 and 1.327, respectively, followed by SI (0.964 and 1.083) and sampling synchronization (0.223 and 0.248). This indicated that Fs and SI are crucial for minimizing prediction error and thus play a pivotal role in accurately characterizing the pulse artifact. The results of this study enable focusing some of the study design parameters to minimize TMS pulse artifact, which is essential for both enhancing the reliability of clinical TMS-EEG applications and improving the overall integrity and interpretability of TMS-EEG data.**

***Index Terms*— TMS-EEG, pulse artifact, stimulation intensity, sampling frequency, synchronization.**

I. Introduction

TRANSCRANIAL magnetic stimulation (TMS) [1] is a non-invasive brain stimulation technique that employs electromagnetic pulses to modulate neuronal activity through the scalp, thereby offering insights into the functioning and structural integrity of the brain [2]. The integration of TMS with various neuroimaging techniques is becoming common for mapping the spatial and temporal properties of the TMS-elicited responses. TMS has been applied alongside computed tomography and magnetic resonance imaging (MRI) to study its connection to the structure of the brain [3]. To investigate the impact of TMS on blood flow, functional MRI, functional near-infrared spectroscopy (fNIRS), and positron emission tomography have proved useful [3], [4]. To assess the neural effects of TMS, electroencephalography (EEG) and magnetoencephalography have been utilized [5].

The coupling of TMS with EEG has been recognized as an important non-invasive modality to investigate the excitability and connectivity patterns of the human cerebral cortex [6], [7]. It has potential applications in clinical diagnostics and neuroscience research [8], [9], [10], [11], [12]. TMS-EEG combines stimulation and high temporal precision recording to allow millisecond-level observation of the propagation of stimulation-evoked neural activity within the brain [13]. TMS-EEG can be integrated effectively both in real-time and offline, offering flexibility to explore the immediate and subsequent effects of brain stimulation [3]. The ability of EEG to capture the electrical activity of the brain by measuring changes as potential difference between electrodes placed on the scalp gives it an edge over other neuroimaging modalities that rely on much slower hemodynamic responses such as fNIRS [14]. This enables for measurement of the precise timing of neural events relative to stimuli as event-related potentials (ERPs) [3].

The accurate interpretation of TMS-EEG data is often obscured by various characteristic artifacts which can be of

Manuscript received 11 December 2023; revised 6 June 2024; accepted 6 July 2024. Date of publication 18 July 2024; date of current version 25 July 2024. This work was supported in part by the State Research Funding, Kuopio, Finland. The work of Zunaira Jamil, Laura Säisänen, Jusa Reijonen, and Petro Julkunen was supported by the Research Council of Finland under Grant 322423. *(Corresponding author: Zunaira Jamil.)*

This work involved human subjects or animals in its research. Approval of all ethical and experimental procedures and protocols was granted by Research Ethics Committee of Kuopio University Hospital under Application No. 59/2012.

Zunaira Jamil, Laura Säisänen, Jusa Reijonen, and Petro Julkunen are with the Department of Technical Physics, University of Eastern Finland, 70210 Kuopio, Finland, and also with the Department of Clinical Neurophysiology, Kuopio University Hospital, 70200 Kuopio, Finland (e-mail: zunaira.jamil@uef.fi).

Michal Demjan is with Bittium Biosignals Oy, 70800 Kuopio, Finland, and also with the Department of Clinical Neurophysiology, Kuopio University Hospital, 70200 Kuopio, Finland.

Digital Object Identifier 10.1109/TNSRE.2024.3429176

non-physiological or physiological nature [15], [16]. Non-physiological artifacts, stemming from electromagnetic or mechanical sources, can interfere with the accurate measurement of neural responses. Electromagnetic interference, such as recharge and decay artifacts from capacitor recharging and electrode polarization, can be managed by utilizing TMS-compatible EEG systems, adjusting stimulator configurations, and selecting non-polarizing materials [17], [18]. Differentiating genuine neural responses from TMS-induced artifacts in EEG recordings, especially within the first 50 ms after the TMS pulse, while minimizing the pulse artifact duration and amplitude, remains a challenge [19], [20]. The early components of the TMS-EEG response provide local information of the activated neural population that is at the focus of TMS and hence provide direct information about the local cortical excitability [21]. The observable pulse artifact stems from the application of a time-varying magnetic field of 2–3 T for $\sim$200 μs, which induces an electric field that activates the cortical neurons [22]. This transient, high-amplitude electromagnetic disturbance results in large spikes in the surface EEG, which are several magnitudes greater than typical neural activity, adding further complexity to the analysis process [23]. Despite great efforts to reliably remove the pulse artifact using signal processing techniques [24], [25], [26], [27], it remains an unavoidable consequence of using TMS with EEG. However, its duration can be minimized effectively by using amplifiers with sufficient dynamic range, maintaining an adequate sampling frequency (Fs), and employing a sufficient cut-off frequency for the anti-aliasing filters [17], [28].

Stimulation and response recording parameters have a critical role in ensuring the safety and effectiveness of the TMS-EEG procedure. The stimulation intensity (SI) serves as a key parameter that significantly impacts both the validity and interpretability of the experimental results [29]. The motor threshold is often employed as a benchmark for calibrating SIs in TMS experiments [30]. Lower SIs often yield subthreshold neural modulations with higher spatial specificity [31], but may produce weaker signals that are more difficult to distinguish from noise in EEG, resulting in a low signal-to-noise ratio. In contrast, high-intensity stimulation can recruit larger and deeper brain areas, including connecting pathways and subcortical structures [32], which may result in more robust EEG signals at the cost of increased risk of side effects, such as discomfort [33]. Furthermore, the choice of Fs of the EEG recording is pivotal for data quality and interpretability. A high Fs enhances temporal resolution and signal-to-noise ratio, facilitating advanced signal processing and artifact removal. It also allows for the capture of high-frequency neural events [34]. Conversely, a lower Fs may miss rapid neural dynamics [35] and complicate artifact rejection [17]. The timing of TMS with respect to the sampling of EEG signal could affect the characteristics of TMS-induced artifacts [36]. This effect could be minimized by synchronizing the TMS with the EEG sampling. This is accomplished by sending a trigger signal to the EEG system, which then holds the trigger until the next EEG sample is collected before forwarding the trigger to the stimulator to deliver the stimulation. This way, timing of the TMS is coordinated by the EEG acquisition system, ensuring that both the delivery of TMS and the consequent artifacts are in synchrony with the EEG sampling rate [37]. Furthermore, synchronizing TMS with person's individual EEG rhythm has been shown to influence brain activity and responses, offering a novel approach to modulate neural dynamics [38], [39].

Despite the existence of numerous strategies to mitigate the TMS-EEG artifacts [27], [40], [41], [42], [43], it is imperative to have comprehensive understanding of how different parameters, such as the applied SI and Fs, influence the pulse artifact. Moreover, the importance of synchronizing the TMS with EEG sampling is an underexplored domain that could provide additional benefits. It not only holds potential for pulse artifact reduction, but also ensures the reliability of EEG data by minimizing the temporal variability introduced by TMS pulse artifacts in TMS-EEG studies [37].

This study aims to fill gaps related to some of the parameters used in designing TMS-EEG studies by exploring the effects of variations in SI, Fs and TMS pulse synchronization with EEG sampling on TMS pulse artifact. We hypothesize that these parameters can significantly affect the amplitude and duration of the artifact. The findings of the present study will help minimize the appearance of the raw pulse artifact for assuring a good quality recording in future TMS-EEG studies and may also help with the removal of the artifact.

II. Methods

A. Subjects and Data

During the TMS-EEG session, the left primary motor cortex (M1) was stimulated, and EEG data were collected from eight healthy subjects (six right-handed, five males, mean age 31 $\pm$ 5 years). The data for each subject were recorded in a single TMS-EEG session, each lasting for approximately two hours. The study had an approval from the Research Ethics Committee of Kuopio University Hospital (permission number: 59/2012) and was conducted in compliance with the Declaration of Helsinki. Informed consent was taken from all volunteers of the study.

B. Experimental Setup

Prior to the study, each participant underwent structural MRI of the head, which facilitated the use of a navigated brain stimulation system (Nexstim Plc, Helsinki, Finland). EEG was recorded with NeurOne DC-amplifier (Bittium Plc, Kuopio, Finland) with 64 active channels and dynamic range of $\pm$430 mV. In the beginning of the experiments, the electrode contacts were prepared to ensure impedances were $<$5 kΩ. The reference and the ground electrodes were positioned on the forehead. Electro-oculography electrodes were positioned below the left eye and above the right eyebrow. Motor evoked potentials (MEPs) were measured from the right hand first dorsal interosseous (FDI) muscle using the Nexstim electromyography (EMG) system with sampling rate of 3 kHz. Following the placement of the EEG cap, participants received biphasic TMS through a figure-of-eight coil (outer loop diameter of 70 mm). Participants were seated comfortably, asked to remain relaxed, and to keep their eyes open. The major parts of experimental setup have been described in earlier study [44].

TABLE I
SUMMARY OF FINDINGS FOR ELECTRODE C3. THE REPORTED VALUES ARE BASED ON THE GROUP MEAN AVERAGE WITH 95% CONFIDENCE INTERVALS

Sequence number	1	2	3	4	5	6
Stimulation intensity (% rMT)	90	90	120	120	120	120
Sampling frequency (kHz)	20	20	20	5	5	20
Synchronization of TMS with EEG sampling	No	Yes	No	Yes	No	Yes
Amplitude median (mV), (Interval between 2.5th and 97.5th percentiles)	395.1 (371–404)	400.5 (383–411)	384.2 (361–396)	31.9 (23–48)	29.9 (21–404)	389.4 (371–413)
Duration median (ms), (Interval between 2.5th and 97.5th percentiles)	1.8 (1.7–2.8)	2.1 (1.7–2.7)	2.6 (1.8–10.9)	5.0 (4.8–11.2)	5.5 (2.7–11.4)	2.7 (2.0–11.0)
Amplitude coefficient of variation for within-subject variability (95% CI)	0.042 (0.038-0.048)	0.012 (0.011-0.013)	0.040 (0.036-0.045)	0.006 (0.006-0.007)	0.048 (0.043-0.054)	0.011 (0.010-0.012)
Duration coefficient of variation for within-subject variability (95% CI)	0.051 (0.046, 0.057)	0.062 (0.055-0.070)	0.208 (0.187–0.235)	0.118 (0.106–0.133)	0.220 (0.190–0.248)	0.551 (0.495–0.622)

The participants were unaware of the sequences being tested, and the order of the sequences was randomized.

To locate the ideal stimulation site in the left M1 for the right FDI, the precentral gyrus along the central sulcus was stimulated. The orientation of the TMS-induced electric field was adjusted to be perpendicular to the sulcal wall to optimize cortical activation. The specific site that consistently produced the largest and most reliable MEPs in the FDI muscle was designated as the optimal representation area, i.e., the stimulation target [45], [46].

The subsequent experimental protocol was set to deliver 150 single pulses in six repeated TMS-EEG sequences considering the dimensions of SI (either 90% or 120% of resting motor threshold (rMT)), and Fs (either 5 kHz or 20 kHz). Both SI and Fs conditions were paired with EEG sampling synchronized with TMS pulse for three sequences and conventionally under non-synchronized setting for the other three sequences (Table I). All data analyses were performed identically in a semiautomatic manner by the corresponding author.

C. Signal Preprocessing

Preprocessing of the EEG signal was conducted in MATLAB (Version R2022b, MathWorks Inc., Natick, USA) utilizing functions from both EEGLAB 2022.1 [47] and the TMS-EEG signal analyser (TESA) toolbox [22]. To understand the inherent characteristics of the pulse artifact, epochs and channels potentially contaminated with noise were minimally processed. Since EEG data contain trends and drifts that could distort the appearance of the underlying neural dynamics and might affect subsequent analysis, linear detrending of the data was performed within the time window between 0 ms (marking the moment of TMS) and 100 ms to remove DC offset within the primary analyzed time window. The data were then segmented into epochs using a time span between 200 ms before and 500 ms after the stimulation event. Artifact- and noise-contaminated data were used in the analysis, assuming that the pulse artifact was the dominant common component in the signal, especially in the vicinity of the stimulation target.

D. Artifact Analysis

The amplitude of the pulse artifact was calculated as peak-to-peak voltage difference where a single peak was characterized as a local maximum denoted by the greatest amplitude across the entire epoch and was flanked by two adjacent minima (Fig.1). This calculation was performed for all electrodes in each trial and was repeated for all 150 trials within a sample. The process was then replicated across all six samples for the subject, providing a comprehensive analysis of the peak-to-peak amplitudes within the dataset.

In the duration analysis of the epoched EEG data, the pre-stimulus waveform was extracted. This waveform was based on specific time indices corresponding to the period preceding the stimulation event, where no significant stimulus-coupled neural activity was expected. Full-wave rectification of the baseline-corrected pre-stimulus waveform was performed uniformly across all electrodes for each individual trial, in order to isolate neural responses from confounding factors. Concurrently, the post-stimulus waveform was extracted corresponding to the related time interval, and the pre-stimulus baseline was subtracted from it. This facilitated the extraction of significant pulse artifact data, commencing from 0 ms onward.

After the preprocessing of the epoched EEG data, the *moving window peak-to-peak amplitude method* [48] was employed to determine the onset and offset of the pulse artifact. A 1-ms window was defined and placed at the beginning of the post-stimulus signal. The window size provided an optimal balance between reliable detection of artifact and avoiding the incorrect marking of background EEG as an artifact. To identify significant deviations, a threshold was defined based on the interquartile range (IQR) of the pre-stimulus signal. The IQR, representing the middle 50% of data, was chosen due to its robustness against outliers in comparison to other range measures such as standard deviation [49], ensuring that the threshold is not unduly influenced by extreme values [50]. This threshold was set as three times the IQR based on Empirical Rule – a.k.a. 68-95-99.7 rule [51]. Following this rule, in a normally distributed set of data (such as baseline noise), about 68% of the data falls within one standard deviation (SD) of the mean, about 95% falls within two SD, and about 99.7% falls within three SD. The defined window was systematically slid through the data, scanning for peaks that exceeded the predefined threshold.

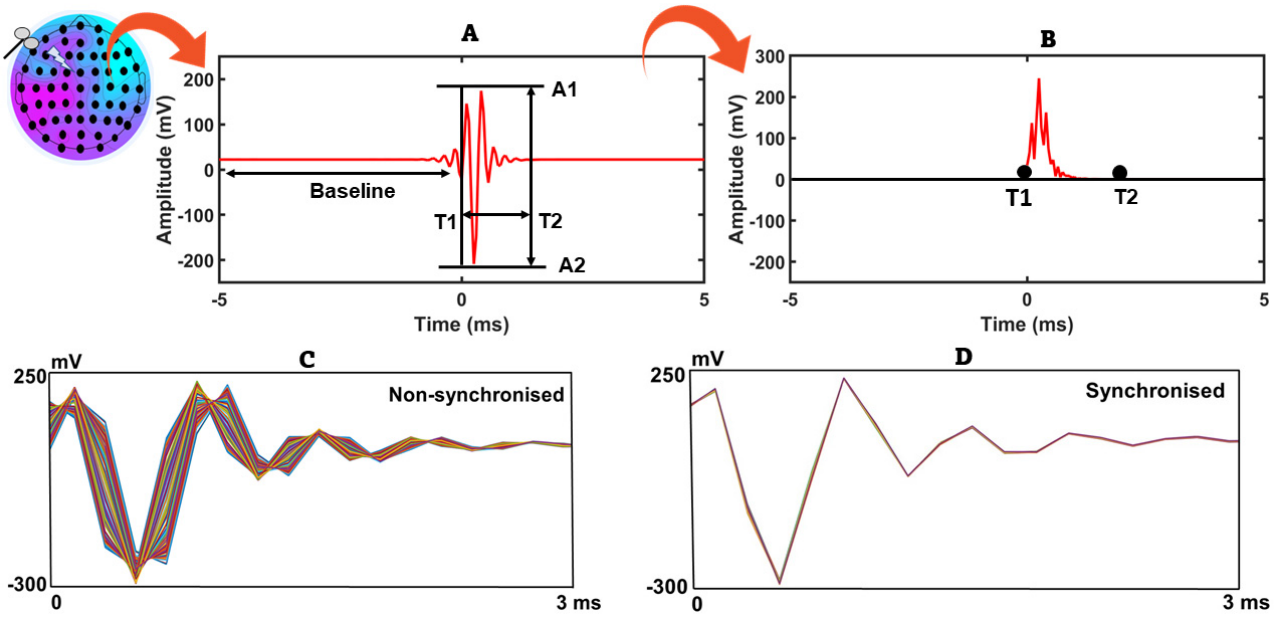

Fig. 1. A) TMS-EEG pulse artifact, with peak-to-peak amplitude denoted by A1 and A2, and duration denoted by T1 and T2. Stimulus is given at time 0 ms. B) The onset and offset times of the pulse artifact. The artifact initiates concurrently with the stimulation represented by T1 and dissipates ~2 ms post-stimulus represented by T2. C) Non-synchronized TMS-EEG trials. D) Synchronized TMS-EEG trials. The TMS pulse is synchronized with the sampling frequency of the EEG acquisition device, which serves as the basis for trial synchronization.

For each individual trial, the onset of the pulse artifact was identified by detecting the first 1-ms window where the signal amplitude value surpassed the threshold. Upon satisfying this condition, the onset time was documented, and the search proceeded to find the offset of the artifact. The offset of the artifact was documented where the signal amplitude value descended below the threshold. This process continued until the whole post-stimulus epoch had been tested. The duration of each artifact was obtained by subtracting the offset time from the onset for every electrode and trial. Finally, the median artifact duration was calculated for each electrode, considering the artifact durations across all trials for that particular electrode. In Fig.1, we illustrate the methodology used to define the temporal boundaries of the pulse artifact employing the moving window peak-to-peak amplitude method.

E. Statistical Analysis

To analyze the central tendency of the data, statistical measures including the median, variance, and percentiles (from 2.5th to 97.5th) were computed for the 64 EEG electrodes (excluding the electro-oculogram and electrocardiogram electrodes), for both peak-to-peak amplitude and artifact duration in each sample.

The distributions of peak-to-peak amplitude and duration of the pulse artifact were examined employing both visual inspection techniques, such as histograms and quantile-quantile (Q-Q) plots, and Kolmogorov-Smirnov test. The results indicated a non-normal, bimodal distribution for the peak-to-peak amplitude and a non-normal distribution for the artifact duration. The paired Wilcoxon signed-rank tests were conducted to examine the effects of specific experimental conditions, defined by SI and Fs: [SI = 90% rMT & Fs = 20 kHz], [SI = 120% rMT & Fs = 5 kHz], and [SI = 120% rMT & Fs = 20 kHz]. For each condition, median values for both artifact peak-to-peak amplitude and duration were analyzed to determine whether synchronized and non-synchronized settings yielded statistically different outcomes.

Since the data did not align with any specific conventional distribution, machine learning techniques were employed avoiding any assumption on the underlying data distribution. A random forest regression model was trained on the processed data to predict the response variables, which were the median values of the peak-to-peak amplitudes and the durations of the pulse artifact. The random forest, characterized by its non-parametric and ensemble-based approach, was less prone to overfitting due to its robust predictive capability especially when dealing with small sample size and in the presence of outliers [52], [53]. The median values for the response variables were calculated for each electrode individually, thereby eliminating biases introduced by pooling data across multiple electrodes.

The model employed SI, Fs, and synchronization as predictor variables. For each split in each tree, a random subset of the predictor variables was chosen to find the best split. Predictions from individual trees were averaged for regression to create the final prediction. The model was created using a forest comprised of 500 individual decision trees. The hyperparameter tuning of the trees was done using the grid search method by iterating over a predefined set of values for the number of trees, fitting the model, and selecting the number of trees that results in the smallest out-of-bag (OOB) permuted variable delta error. This measure reflects each variable's contribution to the model's predictive accuracy.

Bootstrap Sampling was performed additionally for more robust and nuanced understanding of variable importance. Variable importance quantified the contribution of each

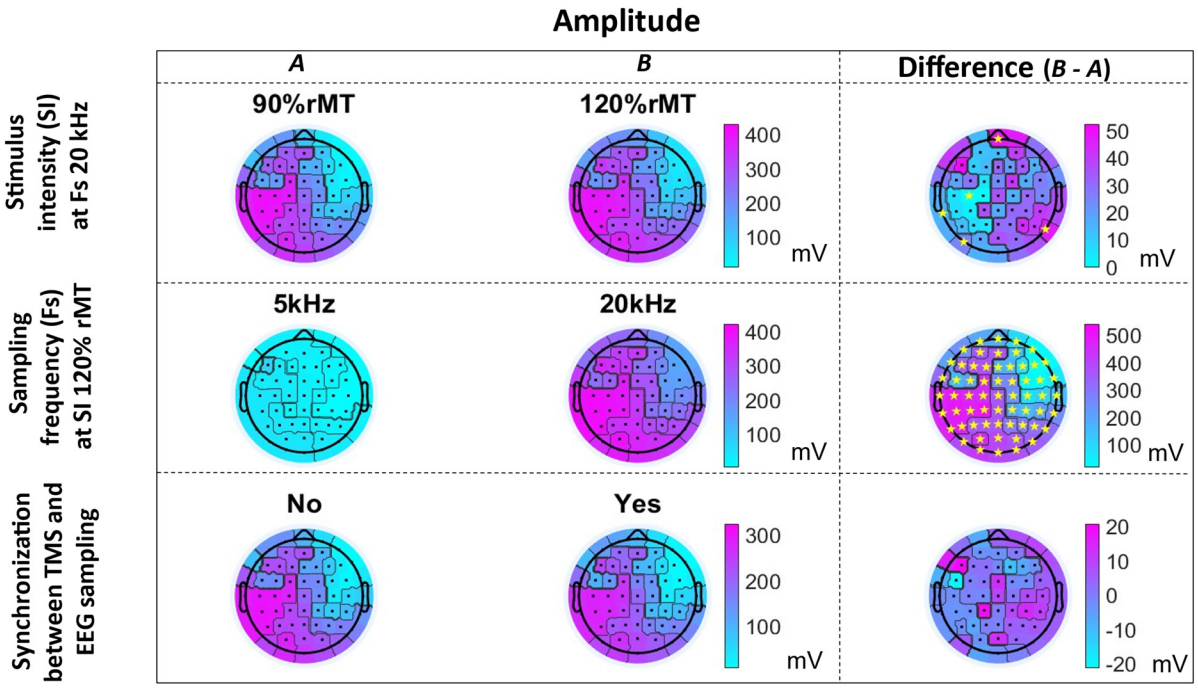

Fig. 2. Topographical distribution of TMS pulse artifact amplitude across different experimental conditions, including (first row) stimulation intensity (90% rMT and 120% rMT) at sampling frequency of 20 kHz, (second row) sampling frequency (5 kHz and 20 kHz) at stimulation intensity of 120% rMT, and (third row) synchronization between stimulation and EEG sampling (No/Yes). The row within each condition displays the mean artifact amplitude, measured in millivolts (mV). The 'Difference' column highlights the difference (B-A) in artifact amplitude between the conditions, with the color intensity denoting the magnitude of the difference. The yellow stars indicate significant differences ($p< 0.05$) in the corresponding location derived from the Wilcoxon rank sum test.

predictor variable to the predictive accuracy of the model. It measured how much the model's prediction error increased when the data for that variable was permuted randomly while all other variables were held constant. 1000 bootstrap samples were drawn (with replacement) from the original data and a new random forest regression model was trained on each sample. The variable importance was recalculated for each model, allowing to assess the stability of importance scores across different samples from the same population. The 2.5th and 97.5th percentiles of the bootstrapped importance values were calculated to form 95% confidence interval (CI) for each variable's importance.

Topological visualizations of data distribution for peak-to-peak amplitudes and artifact durations were generated using nearest neighbor interpolation. For each unique electrode, data were segregated based on specific stimulation parameter conditions. Average values were determined for each electrode under each condition and topographical plots were generated. The p-values were obtained using the Wilcoxon rank sum test and were adjusted for multiple comparisons utilizing the false discovery rate. To control the increased risk of type I errors due to multiple comparisons across the large number of electrodes, p-values were adjusted using the Benjamini-Hochberg False Discovery Rate (FDR) method. This adjustment was applied spatially across all electrodes for each set of conditions.

III. Results

Topographical plots that summarize the effect of the investigated parameters, i.e., SI, Fs and synchronization, on the pulse artifact amplitude and duration are shown in Figs. 2 and 3, respectively. Neither the amplitude nor the duration data were normally distributed ($p < 0.001$, Kolmogorov-Smirnov test). The paired Wilcoxon signed-rank tests indicated that for most conditions, both peak-to-peak amplitude and artifact duration showed significant differences between synchronized and non-synchronized conditions, i.e. with SI=90% rMT and Fs=20 kHz, as well as SI=120% rMT and Fs=20 kHz ($p < 0.001$). The analysis revealed a significant difference in the peak-to-peak amplitudes between synchronized and non-synchronized condition, with amplitudes being 3% lower in synchronized settings as determined by specific relative percentage differences ($p = 0.0125$). There were no significant differences in artifact durations ($p = 0.2832$) (Fig. 3).

The pulse artifact amplitudes at SI 90% of rMT were on average 21 mV lower than those at 120% of rMT (relative percentage difference: 6%). Also, the amplitude values at Fs of 20 kHz were on average 250 mV higher than those at 5 kHz (relative percentage difference: 86%). The synchronized condition showed pulse artifact amplitude lower on average by 7 mV than that in the non-synchronized condition (relative percentage difference: 3%) (Fig. 2).

The artifacts induced at SI of 120% rMT had an average duration longer by 0.9 ms than at 90% of rMT (relative percentage difference: 30%). The Fs of 20 kHz demonstrated a reduced artifact duration in contrast to the lower Fs of 5 kHz by 2.0 ms (relative percentage difference: 57%). The synchronized condition showed pulse artifact duration longer by 0.2 ms than in the non-synchronized condition (relative percentage difference: 6%), without reaching statistical

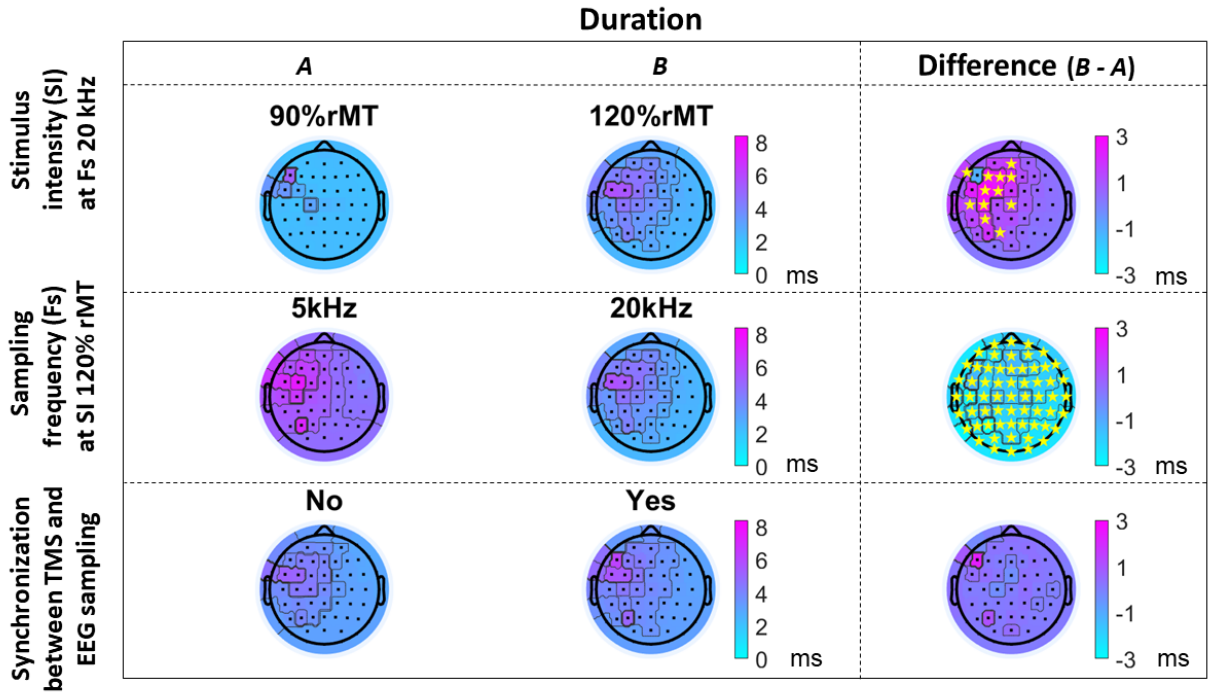

Fig. 3. Topographical distribution of TMS-EEG pulse artifact duration across different experimental conditions, including (first row) stimulation intensity (90% rMT and 120% rMT) at sampling frequency of 20 kHz, (second row) sampling frequency (5 kHz and 20 kHz) at stimulation intensity of 120% rMT and (third row) synchronization between stimulation and EEG sampling (No/Yes). The row within each condition displays the mean artifact duration, measured in milliseconds (ms). The 'Difference' column highlights the difference (B-A) in artifact duration between the conditions, with the color intensity denoting the magnitude of the difference. The yellow stars indicate significant differences ($p< 0.05$) in the corresponding location derived from the Wilcoxon rank sum test.

significance (Fig. 3). Descriptive statistics for one electrode (C3) are given in Table I.

The within-subject variations in artifact amplitude indicated consistent artifact amplitudes especially with sample synchronization (Table I). The lowest within-subject variations were observed with the low SI and high Fs; the use of synchronization did not affect the consistency of the artifact duration (Table I).

A. Predictor Variable Importance

Bootstrap sampling provided an understanding of the variable importance. The importance of predictor variables SI, Fs and synchronization on the peak-to-peak amplitude (response variable) as derived from the random forest model, is presented in Fig 4. Fs was found to be the most important predictor with absolute median importance value of 1.444 (relative percentage: 56%) along with the 95% CI of [1.329, 1.572]. SI followed with absolute median importance value of 0.964 (relative percentage: 38%) along with the 95% CI of [0.887, 1.050]. Synchronization had the least impact with absolute median importance value of 0.223 (relative percentage: 6%) along with the 95% CI of [0.061, 0.525].

The importance of predictor variables SI, Fs and synchronization on the artifact duration (response variable) as derived from the random forest regression model, is presented in Fig 5. Fs was found to be the most influential predictor with absolute median importance value of 1.327 (relative percentage: 49%) along with the 95% CI of [1.226, 1.445]. SI followed with absolute median importance value of 1.083

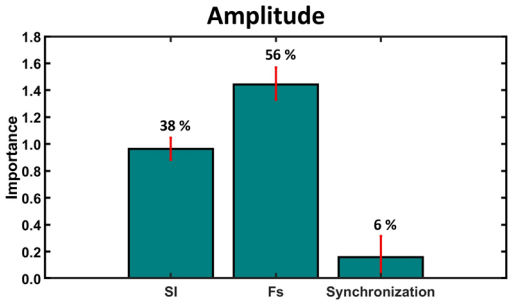

Fig. 4. The relative importance of stimulation intensity (SI), frequency (Fs), and synchronization as predictor variables affecting the amplitude of the pulse artifact. The heights of the bars represent the computed importance, quantified through bootstrapping, with corresponding relative percentages indicated above each bar. The error bars in red indicate confidence intervals.

(relative percentage: 41%) along with the 95% CI of [0.996, 1.176]. Synchronization had the least impact with absolute median importance value of 0.248 (relative percentage: 9%) along with the 95% CI of [0.080, 0.465].

IV. Discussion

The present study investigated the effects of various stimulation parameters on TMS pulse artifact observable in the concurrently recorded EEG. Our results demonstrate that Fs and SI significantly affect the amplitude and duration of pulse artifact. Intriguingly, the level of synchronization between TMS and EEG had only a small effect on the amplitude and duration of the pulse artifact.

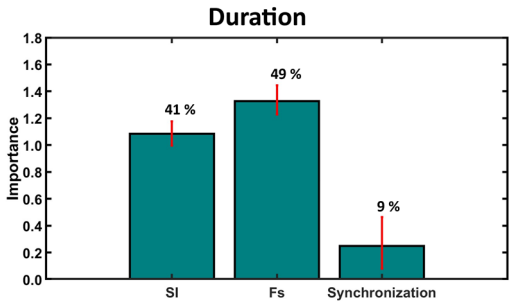

Fig. 5. The relative importance of stimulation intensity (SI), frequency (Fs), and synchronization as predictor variables affecting the duration of the pulse artifact. The heights of the bars represent the computed importance, quantified through bootstrapping, with corresponding relative percentages indicated above each bar. The error bars in red indicate confidence intervals.

A. Sampling Frequency

Expectedly, Fs of 20 kHz exhibited higher peak-to-peak artifact amplitude values compared to the Fs of 5 kHz. This is because some of the high-frequency components of the artifacts were not filtered out by hardware filtering when using the higher Fs. Higher Fs was more adept to capture high-frequency noise or other high-frequency transients. Also, a higher Fs yielded more data points in the same time window and allowed capturing transient peaks or troughs more effectively, leading to larger amplitude values. This impact might have further repercussions on downstream analyses, including signal filtering and identification of event-related potentials [54].

Consistent with previous findings [17], the Fs of 20 kHz demonstrated reduced artifact duration in contrast to Fs of 5 kHz. The present study did not include software filtering which would alter the amplitude characteristics of a signal. If a low-pass filter is applied to data sampled at 20 kHz, the outcome could appear quite similar to the data sampled at 5 kHz.

B. Stimulation Intensity

The pulse artifact amplitudes at SI 90% of rMT were lower than those at 120% of rMT. One of the critical observations in our study was the trade-off between signal clarity and confounding factors in the form of noise, with noise in this context being referred to as random variations in the signal that were devoid of useful information specific to the pulse artifact, particularly when using higher SIs. It is more likely that higher SI may produce a clear, strong signal but it will be at the cost of more artifacts or direct muscle responses [43].

The higher SI induced artifacts of longer durations as compared to lower SI as can be seen in Fig 3 and Table I. An extended artifact duration at higher SI is suggested due to stronger TMS-induced electric field that generates longer interference in the EEG. At higher SIs, there is also the potential for increased discomfort and muscle contractions [21] that might influence the duration of the observed artifact.

C. Synchronization

Synchronization between EEG sampling and TMS appeared to have only a small effect on the amplitude and duration of the artifact when compared to SI and Fs. This suggests that the effects of synchronization are minor. However, the within-subject variation in the TMS-induced artifacts appeared lower (Table I). At this point, we did not test how synchronization might affect the offline removal of the artifact, when it could potentially be more effectively removed due to higher repeatability of the artifact in the time domain. A previous study explored how varying synchronization settings at multiple sampling frequencies (5 kHz, 10 kHz and 20 kHz) affect trial-to-trial variability of the pulse artifact in both phantom and scalp recordings [37]. Our study proceeded further by quantifying how synchronization can affect artifact amplitude and duration along with other experimental conditions (SI and Fs). The previous study aimed to create an artifact template for offline filtering to recover physiological responses, emphasizing the practical application of artifact reduction [37]. Our study quantified the impact of various stimulation parameters using statistical modeling in the form of random forest regression model supported through bootstrapping, providing an empirical basis for understanding the dynamics of pulse artifact.

D. Limitations and Future Directions

One of the limitations of this study was the lack of full factorial design in order to limit the duration of the experiment, and hence fractional design was chosen. Additionally, we did not test the impact of using an AC-coupled amplifier setting on the artifact as generally, DC-coupling is recommended for TMS-EEG experiments [17]. Furthermore, the Fs values used in our study are relatively high compared to those in conventional EEG measurements and they are expected to yield a higher-quality signal than conventional EEG systems. This has allowed enhanced identification of pulse artifact, leading to more detailed and precise artifact analysis. The validity and reliability of the study findings were controlled by bootstrapping tests. Hence, the statistical validity with the present data and the used instrumentation was tested. While the results may be somewhat dependent on the used instrumentation as well as the study population, the general outcome, i.e. the importance of the parameters to the raw pulse artifact characteristics are unlikely to be significantly different, because the agreement between individuals was high (Table I). The reproducibility of the results, e.g. with different systems and study populations, will eventually need to be verified.

To preserve the characteristics of the pulse artifact, including amplitude, shape, and temporal dynamics, only limited preprocessing was applied to the data. Conventional signal preprocessing techniques, such as filtering, might distort or alter the characteristics of the signal. This approach ensured that the raw characteristics of the pulse artifact were maintained, providing a more accurate representation of the artifact. Potential biases in the study include the homogeneity of the subject sample (healthy adults) and repeated measures design where each participant served as their own control. This was done to reduce the variability caused by inter-subject differences and was compensated by replicating samples through bootstrapping.

Despite these limitations, the purpose of our study was to offer optimization suggestions and provide meaningful insights for future TMS-EEG experiment design and artifact

management. Given the observation that a higher Fs produced significantly higher artifact amplitude and reduced artifact duration compared to a lower Fs, future studies could test a wider range of sampling frequencies to determine the optimal Fs that minimizes artifacts while capturing high-quality signals. While the used Fs values were higher than in conventional EEG measurements, it would be valuable to compare results across a spectrum of Fs values to ensure a more general understanding of artifact behavior.

Our findings about the effects of Fs and SI on pulse artifact could inform the design of multi-center studies. One of the significant challenges in neuroscience research is the reproducibility of results. By standardizing how artifacts are managed and how TMS and EEG parameters are set, multi-center studies, each potentially using slightly different equipment and settings, can improve their statistical power and the reproducibility of their findings. Given that individual anatomical differences and TMS coil positioning can introduce variability, using computational models can be instrumental in better understanding of individual brain anatomy and its impact on the pulse artifact. While the present study identified only small effects of synchronization between TMS and EEG sampling on artifact dynamics, it may prove to be a crucial parameter for pulse artifact removal. Future work might go deeper into its potential significance, especially concerning the offline artifact removal processes. There is a need for developing advanced real-time artifact rejection or correction algorithms that leverage machine learning techniques to improve data cleanliness without substantial loss of the neurological signal integrity. Future studies should explore the integration of adaptive filtering techniques based on the study's findings, where filter parameters are dynamically adjusted according to the stimulation intensity and frequency settings.

Given the findings of this study, several recommendations can be made for future TMS-EEG experiment design and artifact management. This study highlighted the role of a higher Fs in capturing more information from the artifact, facilitating more effective removal and recovery. This finding also suggests that conventional EEG systems, which typically operate at lower Fs, might underestimate certain artifact components, thereby skewing data interpretation. Since higher SIs produced clearer responses [55], future studies might investigate a broader range of SIs to identify an optimal value that yields the best signal-to-noise ratio while considering comfort.

E. Conclusion

This study has systematically explored the influence of various stimulation parameters (Fs, SI, and synchronization) on TMS pulse artifact observable in the EEG during TMS-EEG experiments. Our findings reveal that Fs and SI substantially affect both the amplitude and duration of the pulse artifact, highlighting the critical role these parameters play in optimizing TMS-EEG data integrity. The small impact of synchronization suggests that while precise timing between TMS pulses and EEG recordings is beneficial, it is not as critical as the correct setting of Fs and SI for pulse artifact management. Such insights are instrumental in advancing the design and interpretation of future TMS-EEG studies for more standardized and effective experimental frameworks. The path is clear for future research to explore wider parameter ranges and to incorporate adaptive filtering techniques that could dynamically compensate for artifact. Moreover, incorporating consideration of different brain states during experiments might have the potential to provide deeper insights into the optimal conditions for stimulation and recording. This could lead to more personalized and effective therapeutic interventions, tailored to the specific neurophysiological profiles of individuals, thereby expanding the spectrum of possibilities in neuromodulation and TMS-EEG research.

F. Data Availability Statement

The data that support the findings of this study are available on request from the corresponding author. The data are not publicly available.

References

[1] A. T. Barker, R. Jalinous, and I. L. Freeston, "Non-invasive magnetic stimulation of human motor cortex," *Lancet*, vol. 325, no. 8437, pp. 1106–1107, May 1985, doi: 10.1016/S0140-6736(85)92413-4.

[2] J. Rothwell, P. Thompson, B. Day, S. Boyd, and C. Marsden, "Stimulation of the human motor cortex through the scalp," *Experim. Physiol.*, vol. 76, no. 2, pp. 159–200, Mar. 1991.

[3] J. C. Hernandez-Pavon, J. Sarvas, and R. J. Ilmoniemi, "TMS-EEG: From basic research to clinical applications," in *Proc. AIP Conf.*, 2014, pp. 15–21, doi: 10.1063/1.4901355.

[4] H. R. Siebner et al., "Consensus paper: Combining transcranial stimulation with neuroimaging," *Brain Stimulation*, vol. 2, no. 2, pp. 58–80, Apr. 2009, doi: 10.1016/j.brs.2008.11.002.

[5] U. Najib, S. Bashir, D. Edwards, A. Rotenberg, and A. Pascual-Leone, "Transcranial brain stimulation: Clinical applications and future directions," *Neurosurgery Clinics North Amer.*, vol. 22, no. 2, pp. 233–251, Apr. 2011, doi: 10.1016/j.nec.2011.01.002.

[6] L. Fernandez et al., "Cerebral cortical activity following non-invasive cerebellar stimulation—A systematic review of combined TMS and EEG studies," *Cerebellum*, vol. 19, no. 2. Springer, pp. 309–335, Apr. 01, 2020, doi: 10.1007/s12311-019-01093-7.

[7] S. Tremblay et al., "Clinical utility and prospective of TMS–EEG," *Clin. Neurophysiol.*, vol. 130, no. 5, pp. 802–844, May 2019, doi: 10.1016/j.clinph.2019.01.001.

[8] Y. Jin et al., "Therapeutic effects of individualized alpha frequency transcranial magnetic stimulation (TMS) on the negative symptoms of schizophrenia," *Schizophrenia Bull.*, vol. 32, no. 3, pp. 556–561, Sep. 2005, doi: 10.1093/schbul/sbj020.

[9] G. Lanza et al., "A comprehensive review of transcranial magnetic stimulation in secondary dementia," *Frontiers Aging Neurosci.*, vol. 14, Sep. 26, 2022, Art. no. 995000, doi: 10.3389/fnagi.2022.995000.

[10] L. Säisänen et al., "Non-invasive preoperative localization of primary motor cortex in epilepsy surgery by navigated transcranial magnetic stimulation," *Epilepsy Res.*, vol. 92, nos. 2–3, pp. 134–144, Dec. 2010, doi: 10.1016/j.eplepsyres.2010.08.013.

[11] P. Julkunen et al., "Navigated TMS combined with EEG in mild cognitive impairment and Alzheimer's disease: A pilot study," *J. Neurosci. Methods*, vol. 172, no. 2, pp. 270–276, Jul. 2008, doi: 10.1016/j.jneumeth.2008.04.021.

[12] S. Vucic et al., "Clinical diagnostic utility of transcranial magnetic stimulation in neurological disorders. Updated report of an IFCN committee," *Clin. Neurophysiol.*, vol. 150, pp. 131–175, Jun. 01, 2023, doi: 10.1016/j.clinph.2023.03.010.

[13] D. Momi, Z. Wang, and J. D. Griffiths, "TMS-evoked responses are driven by recurrent large-scale network dynamics," *eLife*, vol. 12, Apr. 2023, Art. no. e83232, doi: 10.7554/elife.83232.

[14] W.-C. Su et al., "Simultaneous multimodal fNIRS-EEG recordings reveal new insights in neural activity during motor execution, observation, and imagery," *Sci. Rep.*, vol. 13, no. 1, p. 5151, Mar. 2023, doi: 10.1038/s41598-023-31609-5.

[15] P. C. J. Taylor, V. Walsh, and M. Eimer, "Combining TMS and EEG to study cognitive function and cortico–cortico interactions," *Behavioural Brain Res.*, vol. 191, no. 2, pp. 141–147, Aug. 22, 2008, doi: 10.1016/j.bbr.2008.03.033.

[16] R. J. Ilmoniemi et al., "Dealing with artifacts in TMS-evoked EEG," in *Proc. 37th Annu. Int. Conf. IEEE Eng. Med. Biol. Soc. (EMBC)*, 2015, pp. 230–233, doi: 10.1109/EMBC.2015.7318342.

[17] J. C. Hernandez-Pavon et al., "TMS combined with EEG: Recommendations and open issues for data collection and analysis," *Brain Stimulation*, vol. 16, no. 2, pp. 567–593, Mar. 2023, doi: 10.1016/j.brs.2023.02.009.

[18] F. Farzan, "Transcranial magnetic stimulation–electroencephalography for biomarker discovery in psychiatry," *Biol. Psychiatry*, vol. 95, no. 6, pp. 564–580, Mar. 2024, doi: 10.1016/j.biopsych.2023.12.018.

[19] F. Farzan, M. Vernet, M. M. D. Shafi, A. Rotenberg, Z. J. Daskalakis, and A. Pascual-Leone, "Characterizing and modulating brain circuitry through transcranial magnetic stimulation combined with electroencephalography," *Frontiers Neural Circuits*, vol. 10, p. 73, Sep. 2016, doi: 10.3389/fncir.2016.00073.

[20] J. R. Ives, A. Rotenberg, R. Poma, G. Thut, and A. Pascual-Leone, "Electroencephalographic recording during transcranial magnetic stimulation in humans and animals," *Clin. Neurophysiol.*, vol. 117, no. 8, pp. 1870–1875, Aug. 2006, doi: 10.1016/j.clinph.2006.04.010.

[21] N. C. Rogasch and P. B. Fitzgerald, "Assessing cortical network properties using TMS–EEG," *Hum. Brain Mapping*, vol. 34, no. 7, pp. 1652–1669, Jul. 2013, doi: 10.1002/hbm.22016.

[22] N. C. Rogasch et al., "Analysing concurrent transcranial magnetic stimulation and electroencephalographic data: A review and introduction to the open-source TESA software," *NeuroImage*, vol. 147, pp. 934–951, Feb. 2017, doi: 10.1016/j.neuroimage.2016.10.031.

[23] G. Varone et al., "Real-time artifacts reduction during TMS-EEG co-registration: A comprehensive review on technologies and procedures," *Sensors*, vol. 21, no. 2, p. 637, Jan. 2021, doi: 10.3390/s21020637.

[24] H. Xiong, Y. Di, J. Liu, Y. Han, and Y. Zheng, "A three-dimensional adaptive rational interpolation algorithm for removing TMS-EEG pulse artifacts," *Physiological Meas.*, vol. 44, no. 11, Nov. 2023, Art. no. 115002, doi: 10.1088/1361-6579/ad04b3.

[25] J. C. Hernandez-Pavon et al., "Uncovering neural independent components from highly artifactual TMS-evoked EEG data," *J. Neurosci. Methods*, vol. 209, no. 1, pp. 144–157, Jul. 2012, doi: 10.1016/j.jneumeth.2012.05.029.

[26] S. Atluri et al., "TMSEEG: A MATLAB-based graphical user interface for processing electrophysiological signals during transcranial magnetic stimulation," *Frontiers Neural Circuits*, vol. 10, p. 78, Oct. 2016, doi: 10.3389/fncir.2016.00078.

[27] T. P. Mutanen, J. Metsomaa, M. Makkonen, G. Varone, L. Marzetti, and R. J. Ilmoniemi, "Source-based artifact-rejection techniques for TMS–EEG," *J. Neurosci. Methods*, vol. 382, Dec. 2022, Art. no. 109693, doi: 10.1016/j.jneumeth.2022.109693.

[28] R. J. Ilmoniemi and D. Kicic, "Methodology for combined TMS and EEG," *Brain Topography*, vol. 22, no. 4, pp. 233–248, Jan. 2010, doi: 10.1007/s10548-009-0123-4.

[29] J. Gomez-Tames, I. Laakso, and A. Hirata, "Review on biophysical modelling and simulation studies for transcranial magnetic stimulation," *Phys. Med. Biol.*, vol. 65, no. 24, Dec. 2020, Art. no. 24TR03, doi: 10.1088/1361-6560/aba40d.

[30] J. A. Kaminski, F. M. Korb, A. Villringer, and D. V. M. Ott, "Transcranial magnetic stimulation intensities in cognitive paradigms," *PLoS ONE*, vol. 6, no. 9, Sep. 2011, Art. no. e24836, doi: 10.1371/journal.pone.0024836.

[31] V. Rizzo et al., "Shaping the excitability of human motor cortex with premotor rTMS," *J. Physiol.*, vol. 554, no. 2, pp. 483–495, Jan. 2004, doi: 10.1113/jphysiol.2003.048777.

[32] H. R. Siebner et al., "Transcranial magnetic stimulation of the brain: What is stimulated—A consensus and critical position paper," *Clin. Neurophysiol.*, vol. 140, pp. 59–97, Aug. 2022, doi: 10.1016/j.clinph.2022.04.022.

[33] E. M. Wassermann, "Side effects of repetitive transcranial magnetic stimulation," *Depress Anxiety*, vol. 12, no. 3, pp. 124–129, 2000, doi: 10.1002/1520-6394(2000)12:3<124::AID-DA3>3.0.CO;2-E.

[34] D. Freche, J. Naim-Feil, A. Peled, N. Levit-Binnun, and E. Moses, "A quantitative physical model of the TMS-induced discharge artifacts in EEG," *PLOS Comput. Biol.*, vol. 14, no. 7, Jul. 2018, Art. no. e1006177, doi: 10.1371/journal.pcbi.1006177.

[35] V. Di Lazzaro et al., "Direct demonstration of the effects of repetitive transcranial magnetic stimulation on the excitability of the human motor cortex," *Exp. Brain Res.*, vol. 144, no. 4, pp. 549–553, Jun. 2002, doi: 10.1007/s00221-002-1106-9.

[36] G. Thut, J. R. Ives, F. Kampmann, M. A. Pastor, and A. Pascual-Leone, "A new device and protocol for combining TMS and online recordings of EEG and evoked potentials," *J. Neurosci. Methods*, vol. 141, no. 2, pp. 207–217, Feb. 2005, doi: 10.1016/j.jneumeth.2004.06.016.

[37] L. Tomasevic, M. Takemi, and H. R. Siebner, "Synchronizing the transcranial magnetic pulse with electroencephalographic recordings effectively reduces inter-trial variability of the pulse artefact," *PLoS ONE*, vol. 12, no. 9, Sep. 2017, Art. no. e0185154, doi: 10.1371/journal.pone.0185154.

[38] M. S. George et al., "EEG synchronized left prefrontal transcranial magnetic stimulation (TMS) for treatment resistant depression is feasible and produces an entrainment dependent clinical response: A randomized controlled double blind clinical trial," *Brain Stimulation*, vol. 16, no. 6, pp. 1753–1763, Nov. 2023, doi: 10.1016/j.brs.2023.11.010.

[39] P. C. Gordon et al., "Prefrontal theta-phase synchronized brain stimulation with real-time EEG-triggered TMS," *Frontiers Hum. Neurosci.*, vol. 15, Jun. 2021, Art. no. 691821, doi: 10.3389/fnhum.2021.691821.

[40] P. Julkunen et al., "Efficient reduction of stimulus artefact in TMS–EEG by epithelial short-circuiting by mini-punctures," *Clin. Neurophysiol.*, vol. 119, no. 2, pp. 475–481, Feb. 2008, doi: 10.1016/j.clinph.2007.09.139.

[41] D. Veniero, M. Bortoletto, and C. Miniussi, "TMS-EEG co-registration: On TMS-induced artifact," *Clin. Neurophysiol.*, vol. 120, no. 7, pp. 1392–1399, Jul. 2009, doi: 10.1016/j.clinph.2009.04.023.

[42] H. Sekiguchi, S. Takeuchi, H. Kadota, Y. Kohno, and Y. Nakajima, "TMS-induced artifacts on EEG can be reduced by rearrangement of the electrode's lead wire before recording," *Clin. Neurophysiol.*, vol. 122, no. 5, pp. 984–990, May 2011, doi: 10.1016/j.clinph.2010.09.004.

[43] N. C. Rogasch, R. H. Thomson, Z. J. Daskalakis, and P. B. Fitzgerald, "Short-latency artifacts associated with concurrent TMS–EEG," *Brain Stimulation*, vol. 6, no. 6, pp. 868–876, Nov. 2013, doi: 10.1016/j.brs.2013.04.004.

[44] S. Määttä et al., "Development of cortical motor circuits between childhood and adulthood: A navigated TMS-HdEEG study," *Hum. Brain Mapping*, vol. 38, no. 5, pp. 2599–2615, May 2017, doi: 10.1002/hbm.23545.

[45] P. Julkunen, "Methods for estimating cortical motor representation size and location in navigated transcranial magnetic stimulation," *J. Neurosci. Methods*, vol. 232, pp. 125–133, Jul. 2014, doi: 10.1016/j.jneumeth.2014.05.020.

[46] L. Säisänen et al., "Motor potentials evoked by navigated transcranial magnetic stimulation in healthy subjects," *J. Clinical Neurophysiol.*, vol. 25, no. 6, pp. 367–372, 2008.

[47] A. Delorme and S. Makeig, "EEGLAB: An open source toolbox for analysis of single-trial EEG dynamics including independent component analysis," *J. Neurosci. Methods*, vol. 134, no. 1, pp. 9–21, Mar. 2004, doi: 10.1016/j.jneumeth.2003.10.009.

[48] S. J. Luck, *An Introduction to the Event-Related Potential Technique*, 2nd ed. Cambridge, U.K.: MIT Press, 2014.

[49] C. Leys, C. Ley, O. Klein, P. Bernard, and L. Licata, "Detecting outliers: Do not use standard deviation around the mean, use absolute deviation around the median," *J. Exp. Social Psychol.*, vol. 49, no. 4, pp. 764–766, Jul. 2013, doi: 10.1016/j.jesp.2013.03.013.

[50] D. Ngo et al., "An exploratory data analysis of electroencephalograms using the functional boxplots approach," *Frontiers Neurosci.*, vol. 9, p. 282, Aug. 2015, doi: 10.3389/fnins.2015.00282.

[51] F. Moncada, V. M. Gonzalez, V. Alvarez, B. Garcia, and J. R. Villar, "A preliminary study on automatic detection and filtering of artifacts from EEG signals," in *Proc. IEEE Symp. Comput.-Based Medical Syst.* Piscataway, NJ, USA: Institute of Electrical and Electronics Engineers, Jun. 2021, pp. 420–425, doi: 10.1109/CBMS52027.2021.00046.

[52] G. Biau and E. Scornet, "A random forest guided tour," *Test*, vol. 25, no. 2, pp. 197–227, Jun. 2016, doi: 10.1007/s11749-016-0481-7.

[53] P. Krennmair and T. Schmid, "Flexible domain prediction using mixed effects random forests," *J. Roy. Stat. Soc. Ser. C, Appl. Statist.*, vol. 71, no. 5, pp. 1865–1894, Nov. 2022, doi: 10.1111/rssc.12600.

[54] Y. Li et al., "High-frequency rTMS over the left DLPFC improves the response inhibition control of young healthy participants: An ERP combined 1H-MRS study," *Frontiers Psychol.*, vol. 14, May 2023, Art. no. 1144757, doi: 10.3389/fpsyg.2023.1144757.

[55] M. A. Hays et al., "Towards optimizing single pulse electrical stimulation: High current intensity, short pulse width stimulation most effectively elicits evoked potentials," *Brain Stimul.*, vol. 16, no. 3, pp. 772–782, 2023, doi: 10.1016/j.brs.2023.04.023.